Inorganic Chemistry

Article

pubs.acs.org/IC

tert-Butyl Hydroperoxide Oxygenation of Organic Sulfides Catalyzed by Diruthenium(II,III) Tetracarboxylates

Leslie Villalobos,[†] Julia E. Barker Paredes,[‡] Zhi Cao,[†] and Tong Ren*[,†]

[†]Department of Chemistry, Purdue University, West Lafayette, Indiana 47907, United States

[‡]School of Science and Technology, Georgia Gwinnett College, Lawrenceville, Georgia 30043, United States

Supporting Information

ABSTRACT: Diruthenium(II,III) carboxylates $Ru_2(esp)_2Cl$ (**1a**), $[Ru_2(esp)_2(H_2O)_2]BF_4$ (**1b**), and $Ru_2(OAc)_4Cl$ (**2**) efficiently catalyze the oxygenation of organic sulfides. As noted in a previous work, **1a** is active in oxygenation of organic sulfides with *tert*-butyl hydroperoxide (TBHP) in CH_3CN. Reported herein in detail is the oxygenation activity of **1a**, **1b**, and **2**, with the latter being highly selective in oxo-transfer to organic sulfides using TBHP under ambient conditions. Solvent-free oxidation reactions were achieved through dissolving **1a** or **1b** directly into the substrate with 2 equiv of TBHP, yielding TOF up to 2056 h^{-1} with **1b**. Also examined are the rate dependence on both catalyst and oxidant concentration for reactions with catalysts **1a** and **2**. $Ru_2(OAc)_4Cl$ may be kinetically saturated with TBHP; however, $Ru_2(esp)_2Cl$ does not display saturation kinetics. By use of a series of para-substituted thioanisoles, linear free-energy relationships were established for both **1a** and **2**, where the reactivity constants (ρ) are negative and that of **1a** is about half that of **2**. Given these reactivity data, two plausible reaction pathways were suggested. Density functional theory (DFT) calculation for the model compound $Ru_2(OAc)_4Cl$·TBHP, with TBHP on the open axial site, revealed elongation of the O−O bond of TBHP upon coordination.

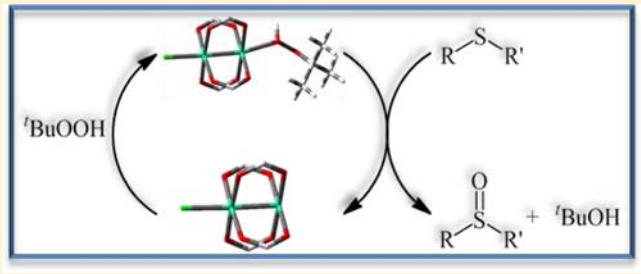

INTRODUCTION

Metal-catalyzed oxygenation of organic compounds is an important synthetic tool in organic chemistry, and performing this type of reaction with inexpensive oxidants or under organic-solvent-free and/or environmentally friendly conditions is highly sought after. Although less explored than C−H oxidation and epoxidation reactions, catalytic oxygenation of organic sulfides plays an important role in the preparation of chiral sulfoxides as synthetic intermediates[1] and desulfurization in fossil fuel upgrading.[2] Additionally, decontamination of chemical warfare agents, such as mustard gas and V-agents, through sulfide oxygenation remains topical.[3] Recent efforts from our group have resulted in several catalytic systems effective in oxygenation of organic sulfides with an array of oxygen donors: H_2O_2 with Me_3TACN-Mn[4] and $[SiW_{10}O_{34}(H_2O)_2]^{4-}$,[5] *tert*-butyl hydroperoxide (TBHP) with Me_3TACN-Mn[6] and $Ru_2(ONHCCR)_4Cl$,[7] and O_2 with $Ru_2(O_2CR)_3(CO_3)$.[8]

It is well-established that, in terms of organic sulfide oxygenation, the general reactivity of common oxygen donors is in the following order: peracid > H_2O_2 > hydroperoxide (ROOH).[9] Nevertheless, *tert*-butyl hydroperoxide is considered an ideal oxidant for field decontamination of chemical agents because of its thermal robustness and biodegradability, but it is difficult to activate and less studied. The first report of catalytic sulfide oxygenation by TBHP was a brief paper by Kuhnen,[10] where methyl phenyl sulfide (MPS, also known as thioanisole) was converted to the corresponding sulfone with the aid of $Mo(acac)_3$. A more efficient sulfide oxygenation by TBHP was achieved by use of $MeReO(mtp)PPh_3$ [mtp = 2-(mercaptomethyl)thiophenol], which yielded a remarkable TOF (turnover frequency) of 200 h^{-1}.[11] Doyle and co-workers[12] have provided many interesting examples of TBHP activation with $Rh_2(cap)_4$ (cap = caprolactamate) in allylic, benzylic, and secondary amine oxidation reactions. Inspired by Doyle's success, our laboratory started to explore the catalytic proficiency of diruthenium species, and reported preliminary findings on sulfide oxygenation with TBHP promoted by $Ru_2(esp)_2Cl$ (**1a**, esp = tetramethyl-1,3-benzenedipropionate, Chart 1).[13] Reported in this Article is the TBHP oxygenation of organic sulfides catalyzed by $Ru_2(esp)_2Cl$ (**1a**), $[Ru_2(esp)_2(H_2O)_2](BF_4)$ (**1b**), and $Ru_2(OAc)_4Cl$ (**2**), related kinetics studies, mechanistic discussion, and density functional theory (DFT) simulation of a possible reaction intermediate.

RESULTS AND DISCUSSION

Preparation and Characterization of Diruthenium Catalysts. $Ru_2(OAc)_4Cl$ (**2**) was synthesized by the literature procedure.[14] $Ru_2(esp)_2Cl$ (**1a**) was prepared from refluxing $Ru_2(OAc)_4Cl$ with 2.2 equiv of H_2esp (esp = $\alpha,\alpha,\alpha',\alpha'$-tetramethyl-1,3-benzenedipropionate)[15] in H_2O−CH_3OH

Received: June 27, 2013
Published: October 11, 2013

 © 2013 American Chemical Society dx.doi.org/10.1021/ic401588j | *Inorg. Chem.* 2013, 52, 12545−12552

Chart 1. Diruthenium Tetracarboxylate Catalysts

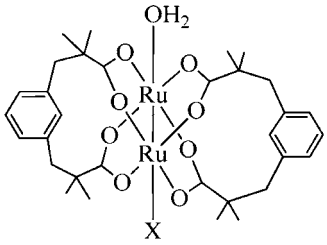

X= Cl (**1a**) and H_2O (**1b**$^+$)

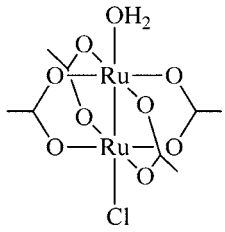

2

(1:2) as previously reported.[13] The reaction between **1a** and silver tetrafluoroborate (2 equiv) yielded $[Ru_2(esp)_2(H_2O)_2]BF_4$ (**1b**). Both compounds **1a** and **1b** were characterized with fast atom bombardment mass spectrometry (FAB-MS) and single-crystal X-ray diffraction study. Similar to previously reported diruthenium(II,III) tetracarboxylates,[16] both $Ru_2(esp)_2Cl$ and $[Ru_2(esp)_2(H_2O)_2]BF_4$ are paramagnetic with room-temperature effective magnetic moments of $3.84\mu_B$ and $3.60\mu_B$, respectively, which correspond to a $S = {}^3/_2$ ground state. The vis−NIR absorption spectra of compounds **1a** and **1b** feature peaks at ca. 467 and 435 nm, respectively, which are attributed to the $\pi(Ru{-}O, Ru_2) \rightarrow \pi^*(Ru_2)$ transition.[17]

Structural detail of molecule **1a** was reported previously.[13] Similar to other reported $M_2(esp)_2$ species,[15,18] **1a** adopts the paddlewheel motif. Also noteworthy is the presence of the axially bound water molecule. The structural plot of **1b**$^+$ and selected key geometric parameters are provided in Figure 1. It is

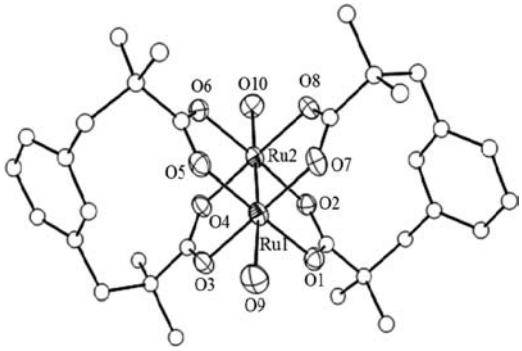

Figure 1. Structural plot of $[Ru_2(esp)_2(H_2O)_2]^+$ cation. Hydrogen atoms were omitted for clarity. Selected bond lengths (in angstroms) and angles (in degrees): Ru1−Ru2, 2.2551(4); Ru1−O9, 2.282(2); Ru2−O10, 2.254(3); Ru1−O1, 2.031(2); Ru1−O3, 2.012(2); Ru1−O5, 2.023(2); Ru1−O7, 2.029(2); Ru2−O2, 2.024(2); Ru2−O4, 2.015(2); Ru2−O6, 2.014(2); Ru2−O8, 2.025(2); Ru(2)−Ru(1)−O(9), 179.08(8); O(10)−Ru(2)−Ru(1), 174.77(8).

clear that $[Ru_2(esp)_2(H_2O)_2]^+$ retains the same paddlewheel core geometry as that observed for its parent compound **1a**. The Ru−Ru bond length of **1b**$^+$ [2.2551(4) Å] is shorter than that of **1a** [2.2768(6) Å], consistent with the removal of the axial chloro ligand that weakens the σ(Ru−Ru) bond by competing for the Ru d_{z^2} orbital. The $Ru{-}O_{ax}$ distances in **1b**$^+$ are also shorter than those of **1a** due to the cationic nature of the Ru_2 core. On the other hand, the $Ru{-}O_{eq}$ distances in **1b**$^+$ and **1a** are comparable. The Ru−Ru bond length of **1b**$^+$ [2.2551(4) Å] is also slightly shorter than that of $[Ru_2(OAc)_4(H_2O)_2]^+$ [2.2648(9) Å].[19]

Diruthenium(II,III) Tetracarboxylates as *tert*-Butyl Hydroperoxide Activators. The initial examination of TBHP oxygenation of organic sulfides was based on **1a**, and sulfides examined include methyl phenyl sulfide (MPS), diphenyl sulfide (PPS), ethyl phenyl sulfide (EPS), and 2-chloroethyl phenyl sulfide (CEPS) as shown in Scheme 1.

Scheme 1. Oxygenation of Organic Sulfides

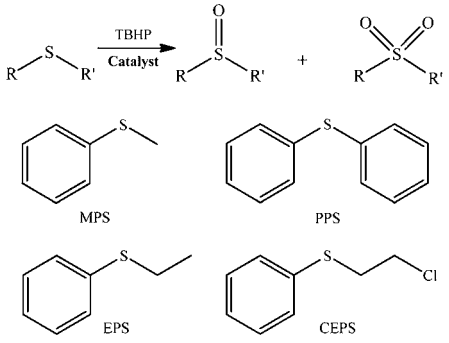

Diruthenium(II,III) Tetracarboxylates as TBHP Activators.

Catalytic reactions performed with methyl phenyl sulfide were monitored with gas chromatography (GC), and the data are presented in Table 1. Contrary to reactions with **1a** and **1b**, reactions with **2** were not performed in CH_3CN. Due to compound insolubility in this solvent, a 1:1 solvent mixture CH_3CN/H_2O was used instead. As shown in entries 1 and 2, $Ru_2(esp)_2Cl$ is active for the oxygenation of MPS with 8 equiv of TBHP. Furthermore, the formation of methyl phenyl sulfoxide was dominant even with TBHP in significant excess. With a catalyst loading of 1 mol %, MPS was consumed in 24 h to yield 70% sulfoxide and 30% sulfone, which corresponds to a TOF of 5 h^{-1}.

Catalytic proficiency of **1a** was further examined forh the TBHP oxygenation of PPS, EPS, and CEPS under the same conditions as those for the MPS reaction. As shown in Table 1, the reactivity of PPS is comparable to that of MPS in terms of both the rate (TOF) and distribution of products. In contrast, oxygenations of both CEPS and EPS were slow and resulted in large amounts of byproducts, similar to previous studies of H_2O_2 and TBHP oxygenation facilitated by Mn-TACN catalysts.[4,6] The formation of elimination products such as phenyl vinyl sulfoxide is attributed to the formation of a sulfenium intermediate via a SET (single electron transfer) mechanism. For compound **1b**, faster oxo-transfer is observed, which is accompanied by an increase in the amount of sulfone produced, as shown in entries 9−12 with both MPS and PPS as substrates.

The above-mentioned TBHP activation by **1a** and **1b** prompted the examination of $Ru_2(OAc)_4Cl$ as a TBHP activator through the oxygenation reactions of both MPS and PPS. As clearly shown by the data in Table 1, $Ru_2(OAc)_4Cl$ is also active in oxygenations of both MPS and PPS. Furthermore, $Ru_2(OAc)_4Cl$ is more efficient in converting MPS than $Ru_2(esp)_2Cl$ but less so in converting PPS.

Good solubility of catalysts **1a** and **1b** in polar organic liquid renders the possibility fo performing catalytic reactions without solvent(s). This aspect was examined with reactions of 8 mmol of MPS as the substrate, 0.05 mol % catalyst, and 2 equiv of TBHP. The solvent-free reactions proceeded much faster than the reactions in CH_3CN, with TOF up to 2056 h^{-1} with **1b** in

dx.doi.org/10.1021/ic401588j | *Inorg. Chem.* 2013, 52, 12545−12552

Table 1. Catalytic *tert*-Butyl Hydroperoxide Oxygenation of Organic Sulfides with 1a, 1b, and 2[a]

entry	RSR′	time (h)	RSR′ (%)	RS(O)R′ (%)	RS(O)$_2$R′ (%)	others	TOF[b]
			Catalyzed by $Ru_2(esp)_2Cl$ (**1a**)				
1	MPS	1	82	15	3	0	20
2	MPS	24	<1	70	29	0	5
3	PPS	12	8	82	10	0	8.5
4	PPS	24	117	74	19	0	5
5	EPS	2	96	1	2	1	1.5
6	EPS	48	9	45	20	26	
7	CEPS	4	84	4,[c] 3[d]		9[e]	2
8	CEPS	48	29	11,[c] 24[d]	2	24[e], 10	
			Catalyzed by $[Ru_2(esp)_2(H_2O)_2]BF_4$ (**1b**)				
9	MPS	2	0	28	71	0	85
10	MPS	6	0	1	99	0	33
11	PPS	2	0	72	28	0	64
12	PPS	6	0	53	45	0	24
			Catalyzed by $Ru_2(OAc)_4Cl$ (**2**)				
13	MPS	2	3	95	2	0	50
14	MPS	4	3	88	8	0	26
15	PPS	1	61	37	2	0	41
16	PPS	12	48	48	4	0	5
17	EPS	6	0	53	21	26	16

[a]Reactions conditions: 1.25 mmol of substrate, 10 mmol of TBHP, 0.0125 mmol of catalyst, room temperature, and 5 mL of the specified solvent(s). [b]Turnover frequency (hour^{-1}) = [RR′SO] + 2[RR′SO$_2$]/[catalyst] × time (in hours). [c]Phenyl disulfide and corresponding sulfoxide. [d]Phenyl vinyl sulfoxide. [e]Chloroethyl phenyl sulfoxide.

1h. Contrary to the reactions inCH_3CN, the product distributions under solvent-free conditions are very similar for both catalysts. For **1a**, the sulfide was completely converted to sulfoxide with less than 1% sulfone. As for **1b**, less than 1% of the sulfide was present with 96% sulfoxide and 3% sulfone (Supporting Information, Table S1). Attempts at solvent-free reactions with **2** provided low rates of conversion, a result ascribed to the poor solubility of the catalyst in MPS.

Because of the selectivity and high TOF of catalysts **1a** and **2**, we were interested in studying reaction kinetics and gaining mechanistic insight of these catalytic reactions. Kinetic data were primarily obtained by monitoring the disappearance of MPS at 290 nm by UV spectroscopy, a technique commonly used in organic sulfide oxygenation reactions.[11,20] Given that the absorbance intensities will vary at different initial MPS concentrations, the pseudo-first-order decay curves were normalized by eq 1

$$\mathrm{Abs}_{290,\mathrm{corr}} = [(\mathrm{Abs}_0 - \mathrm{Abs}_t)/(\mathrm{Abs}_0 - \mathrm{Abs}_\infty)] \quad (1)$$

where Abs_0, Abs_t, and Abs_∞ are the absorbances at 290 nm for a reaction mixture at its initiation, at any given time during the reaction, and the time in which a baseline has been achieved for the reaction, respectively. Reactions followed pseudo-first-order kinetics at various amounts of oxidant and catalyst concentration. The slope values obtained for $\ln(\mathrm{Abs}_{290})$ versus time were plotted against each of the parameters studied to obtain the respective values for the rate constants.

The dependence on oxidant was analyzed in the presence of 2 mM MPS and $Ru_2(esp)_2Cl$ (**1a**) in CH_3CN. The disappearance of MPS during the first 35 min was monitored for a set of reactions with up to 300 equiv of TBHP, and the reaction was found to be pseudo-first-order after a short lag time (<5 min). The k_{obs} data extracted from the plot of $\ln(\mathrm{Abs}_{290})$ versus time were plotted versus the amount of TBHP in Figure 2, from which a linear fit yielded k_{TBHP}(**1a**) = 3.60×10^{-5} min^{-1}·M^{-1}. Furthermore, the linear dependence

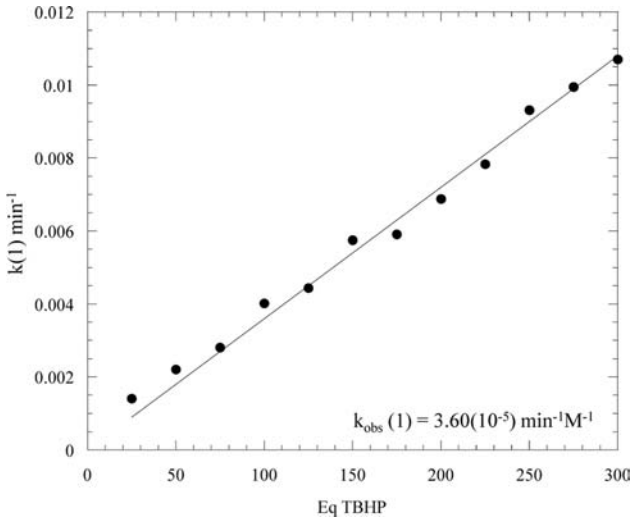

Figure 2. Variation of TBHP in CH_3CN for oxygenation of MPS with $Ru_2(esp)_2Cl$ (**1a**).

was retained with up to 1000 equiv of TBHP (data not shown). Such behavior indicates that the rate of reaction may be diffusion-controlled in the case of $Ru_2(esp)_2Cl$.[21]

The rate dependence on TBHP was also determined in the presence of MPS and **2**. As shown in Figure 3, the rate of reaction increased with increasing TBHP concentration initially but plateaued around 60 equiv of TBHP. Linear fitting of data up to 50 equiv of TBHP yielded k_{TBHP}(**2**) = 3.14×10^{-4} min^{-1}·M^{-1}. Similar saturation behavior was observed in sulfide oxygenation by H_2O_2 with Fe catalysts and was attributed to an oxidizing intermediate with H_2O_2 bound to the catalyst.[22] Likely, TBHP binds to the free axial site (trans to chloro) of $Ru_2(OAc)_4Cl$ readily and contributes to its saturation kinetics. On the other hand, the free axial site in $Ru_2(esp)_2Cl$ is less accessible compared to that of $Ru_2(OAc)_4Cl$, which hinders the

dx.doi.org/10.1021/ic401588j | Inorg. Chem. 2013, 52, 12545−12552

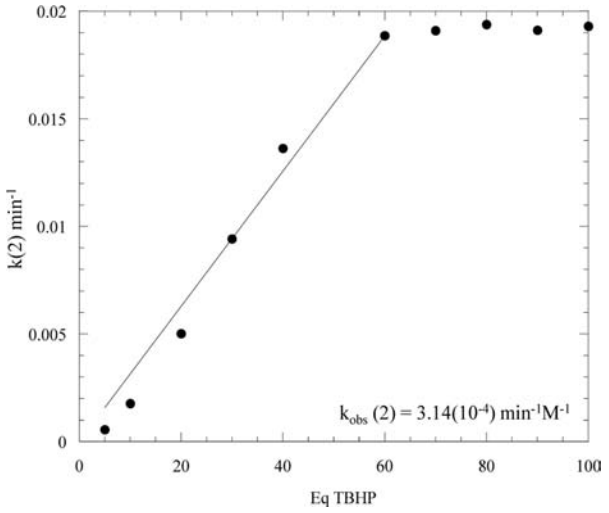

Figure 3. Variation of TBHP for oxygenation of MPS with $Ru_2(OAc)_4Cl$ (**2**) in CH_3CN/H_2O (1:1).

formation of the oxidant-bound intermediate and results in the absence of saturation kinetics.

Dependence of initial rates on catalyst concentration was similarly analyzed by a UV absorption spectrum technique, where the concentration of catalyst was varied in the presence of 2 mM MPS and 200 mM TBHP. Linear dependence of initial rates on the concentration of the catalyst was established for both **1a** (Figure 4) and **2** (Figure S1 in Supporting

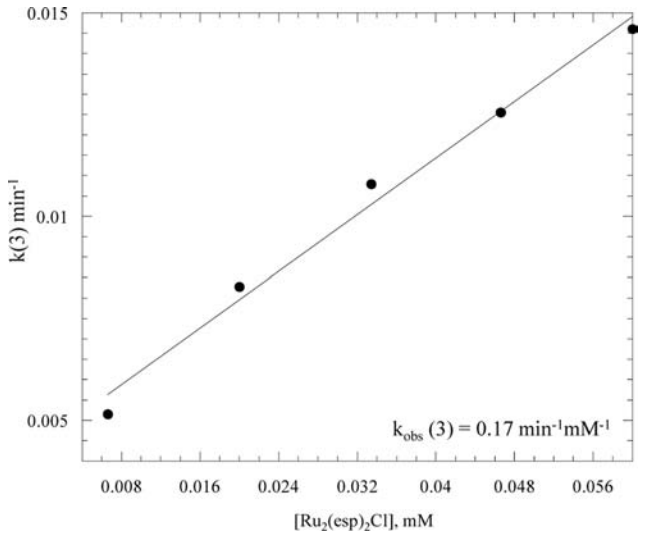

Figure 4. Data analysis of variation of $Ru_2(esp)_2Cl$ (**1a**) in CH_3CN for oxygenation of MPS with TBHP.

Information), with k_{cat} as 0.17 and 0.59 $min^{-1}\cdot mM^{-1}$ for **1a** and **2**, respectively. The fact that the TBHP oxygenation reactions are first-order in catalyst concentration implies a single diruthenium compound as the active species. The nonzero intercept (ca. 0.004 min^{-1}) in Figure 4 corresponds to the rate of noncatalytic sulfide oxygenation reaction, and its magnitude is similar to that found in previous studies.[23] The initial rate of reaction with catalyst **1b** was also determined with [**1b**] = 0.05 mM under the same conditions as those for **1a** and **2**. The k_{obs} determined (0.087 $min^{-1}\cdot M^{-1}$) is about 7 times that for **1a** at the same concentration (Figure S2 in Supporting Information), which is consistent with the much faster sulfide to sulfoxide/sulfone conversation by **1b** than **1a** from the GC data. Compound **1b** has two axial positions available, which results in the interaction of the TBHP molecule with either or both axial sites. With the increase in reaction rate, a decrease in the selectivity was observed.

In order to gain further insight to the mechanism of action of **1a** and **2**, a Hammett plot was constructed by correlating the second-order rate constant with the Hammett constant of the para substituent of thioanisole derivatives.[24] In a typical reaction, 1.0 mM sulfide, 100 equiv of TBHP, and 1.8 mM catalysts were used. These reactions were run in CH_3CN to eliminate the insolubility problem of some MPS derivatives in water. As shown in Figure 5, the reactivity constant (ρ) with

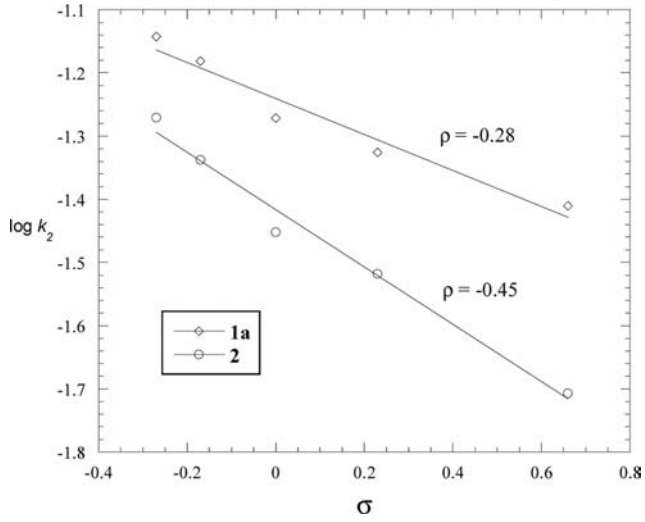

Figure 5. Hammett correlation for the oxygenation of MPS derivatives with catalysts **1a** (◇) and **2** (○). The para substituents are, in ascending order of Hammett constants, -OMe, -Me, -H, -Br, and -CN.

catalyst **1a** is −0.28. In general, a negative ρ value implies a build-up of positive charge in the transition state, and an electrophilically activated peroxo species can be inferred. Vassell and Espenson[20] reported a ρ value of −1.0 for methylrhenium trioxide (MTO) -catalyzed H_2O_2 oxygenation of MPS and derivatives. Takeuchi and co-workers[25] reported a ρ value of −0.42 for the stoichiometric oxygenation of MPS and derivatives by $[Ru(4+)(bpy)_2(O)PR_3]^{2+}$. Clearly, the contrast in ρ between **1a** and MTO is likely attributed to the high formal charge of the latter [Re(7+)]. Similar linear correlation was established for oxygenation reactions catalyzed by **2** as shown in Figure 5, and a reactivity constant of −0.45 was determined. The larger ρ value for $Ru_2(OAc)_4Cl$ suggests that its transition state is more electrophilic than that of **1a,** possibly a reflection of relative electron deficiency of $Ru_2(OAc)_4Cl$.

To gain insight into the electronic interaction between diruthenium(II,III) tetracarboxylate and TBHP, spin-unrestricted DFT calculations were performed on a hypothetical compound **2′**·TBHP, where the free axial position of **2′** is occupied by a TBHP molecule. The geometry of **2′**·TBHP was fully optimized from the crystal structure of **2**·H_2O with a water molecule adjacent to the five-coordinated Ru center being replaced by a TBHP molecule at BP86/LanL2DZ level by using DFT methods (Figure S3 in Supporting Information). The bond lengths and angles around the Ru_2 core in the optimized

dx.doi.org/10.1021/ic401588j | Inorg. Chem. 2013, 52, 12545−12552

geometries are given in Table S2 in the Supporting Information. Figure 6 shows the computed frontier molecular orbital diagrams for compound **2′**·TBHP.

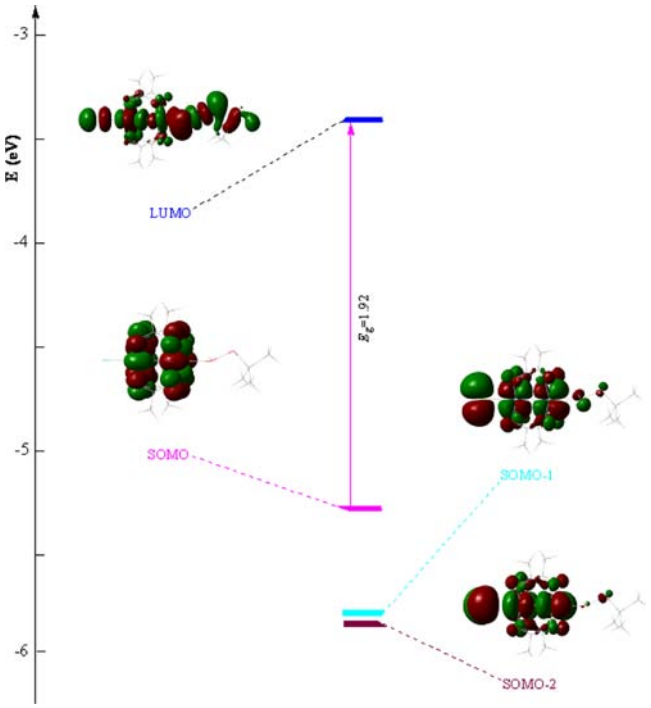

Figure 6. Molecular orbital diagram model compounds **2′**·TBHP obtained from DFT calculations. Only the energy levels for α spin were provided.

DFT calculation for **2′**·TBHP revealed a configuration very similar to that of $Ru_2[ONHCC(CH_3)_2]_4Cl{\cdot}H_2O_2$.[7] With the singly occupied molecular orbital (SOMO), SOMO − 1, and SOMO − 2 being singly occupied, **2′**·TBHP retains a $S = {}^3/_2$ ground state that is common among diruthenium(II,III) compounds.[26] Optimization of **2′**·TBHP with $S = {}^1/_2$ ground state (Figure S4 and Table S4, Supporting Information) resulted in a total energy significantly higher than that with $S = {}^3/_2$, and the $S = {}^1/_2$ ground state was hence deemed unsuitable. It is clear from Figure 6 that the SOMO is predominantly the δ^*(Ru−Ru) orbital with an additional contribution from the lone pairs of O centers of the acetate ligands. The SOMO − 1 and SOMO − 2 are nearly degenerate with a separation of 0.037 eV in **2′**·TBHP, and both are primarily the π^*(Ru−Ru) orbitals with significant contribution of p(Cl) lone pair. Similar to the previous study of H_2O_2 binding to a Ru_2 catalyst, it is likely that the σ-type electron density along the Ru−Ru axial position would be imparted onto TBHP upon its coordination, which leads to a weakened σ(Ru−Ru) and hence more relaxed Ru−Ru bond length, 2.402 Å compared with 2.281 Å in $Ru_2(OAc)_4Cl{\cdot}H_2O$.[16,26] Meanwhile, coordination to Ru_2 also induced significant changes in the geometry of TBHP:[27] the O−O bond was elongated from 1.473 Å in free TBHP to 1.563 Å, and the H−O1−O2−C dihedral angle relaxed from 104.0° to 135.0°, reflecting the conversion of one of the O1 lone pairs into a dative bonding pair. This result implies the important role of the dative coordination of peroxy species to Ru_2 in the eventual O−O bond cleavage.

Mechanistic Consideration. The high utility of TBHP along with the linear dependence on TBHP concentration, demonstrated from kinetic analyses with both $Ru_2(OAc)_4Cl$ and $Ru_2(esp)_2Cl$, suggests that only one TBHP molecule is involved in the transfer of an oxygen to organic sulfide. Linear dependence of catalyst was demonstrated in CH_3CN for both $Ru_2(esp)_2Cl$ and $Ru_2(OAc)_4Cl$, indicating that there is only one diruthenium species involved in each catalytic cycle with diruthenium carboxylate catalysts.

It is reasonable to presume that coordination of TBHP to the vacant axial site and subsequent deprotonation of the coordinated TBHP yields an intermediate $[Cl\text{-}Ru_2(O_2CR)_4\text{-}OO^tBu]^-$. Two plausible pathways of oxo-transfer are shown in Scheme 2. In the first pathway, heterolytic cleavage of O−O

Scheme 2. Possible Oxo-Transfer Mechanisms in TBHP Activation by Ru_2

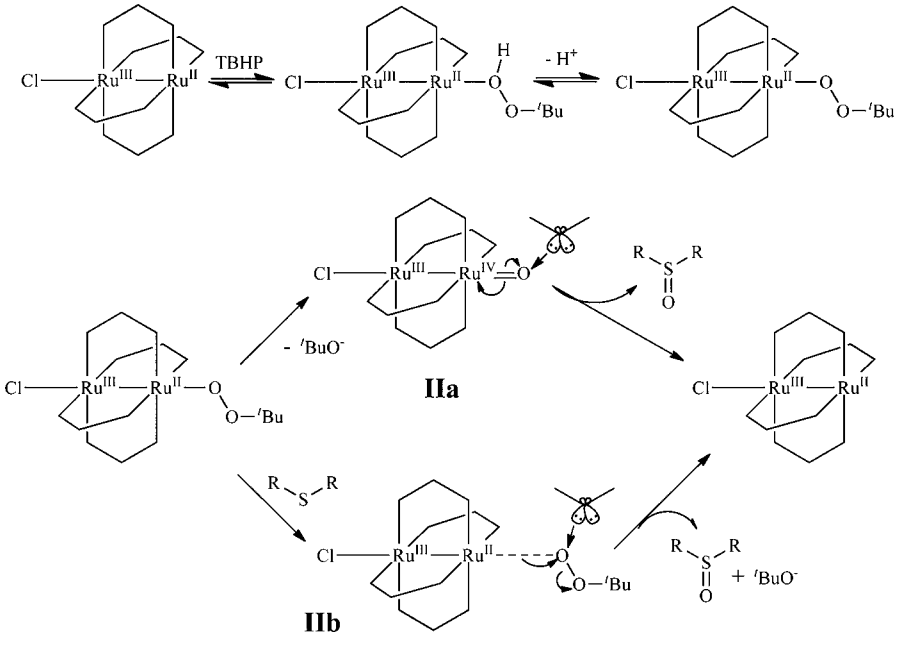

dx.doi.org/10.1021/ic401588j | Inorg. Chem. 2013, 52, 12545−12552

bond in -$O_2{}^t$Bu results in a transient $Ru^{III}-Ru^{IV}=O$ species (**IIa** in Scheme 2), which in turn oxygenates a sulfide substrate. Such a high valent species is plausible when both the frequently observed reversible $Ru_2(+7/+6)$ couple in the cyclic voltammograms of diruthenium alkynyl compounds[28] and the recently observed $Ru_2(7+)$ nitrido species are considered.[29] In the second pathway, the oxo-transfer occurs in a concerted process, where the sulfide substrate reacts with $[Cl\text{-}Ru_2(O_2CR)_4\text{-}OO{}^t\text{Bu}]^-$ directly in the intermediate **IIb**, and the concurrent cleavage of both the O−O bond and a weakened Ru−O bond leads to formation of the corresponding sulfoxide. In the first pathway, the transient oxo species **IIa** is strongly electrophilic due to the higher former charge on the Ru_2 center. The shorter Ru=O distance also necessitates less steric hindrance around the Ru_2 center to enable the approach of a sulfide substrate. Hence, this is likely to be the pathway preferred by $Ru_2(OAc)_4Cl$, which is the more electrophilic catalyst of the two. On the other hand, the peroxy moiety is relatively distant from the Ru_2 center in **IIb**, which allows for the approach of sufide substrate without significant steric crowding. Thus, the concerted pathway is more likely adopted by the bulkier $Ru_2(esp)_2Cl$. The concerted intermediate does not require a significant build-up of positive charge, which is consistent with the smaller ρ value from the Hammett analysis.

Although the mechanisms cannot be proven directly, the observed reactivity is generally consistent. $Ru_2(OAc)_4Cl$ is more selective than $Ru_2(esp)_2Cl$ in the oxygenation of organic sulfides over the corresponding sulfoxides, as expected for a more electrophilic catalyst. Diphenyl sulfide, a substrate that is more sterically hindered, is less reactive in the presence of the catalyst $Ru_2(OAc)_4Cl$ than MPS, but the rate of oxygenation with $Ru_2(esp)_2Cl$ is nearly the same for each substrate.

CONCLUSIONS

The ability of diruthenium(II,III) tetracarboxylate compounds **1** and **2** in promoting oxygenation of organic sulfides by TBHP at ambient conditions has been demonstrated. Solubility of **1a** in polar organic solvent enables facile and selective oxygenation under solvent-free conditions. Both the kinectics data and reactivity pattern pointed to a modestly electrophilic intermediate during the oxygenation catalysis. Currently, we are investigating the feasibility of other organic transformations such as allylic and secondary amine oxidation catalyzed by diruthenium(II,III) tetracarboxylates.

EXPERIMENTAL SECTION

General Information and Materials. TBHP (70% in water), methyl phenyl sulfide (MPS) and 4-(methylthio)benzonitrile were purchased from Sigma−Aldrich (St. Louis, MO). 1-Methoxy-4-(methylthio)benzene, methyl *p*-tolyl sulfide, and 4-bromophenyl methyl sulfide were purchased from Fisher Scientific (Morris Plains, NJ). Acetonitrile was obtained from VWR (Suwanee, GA) and dried over molecular sieves for at least 3 days prior to use. TBHP concentrations were determined by iodometric analysis.[30] Kinetic investigations were performed via spectroscopic absorption spectra on either a Perkin-Elmer Lambda-900 UV−vis−NIR spectrophotometer or a Jasco V-670 spectrophotometer. GC-MS data was obtained on a Hewlett-Packard 5890 series II gas chromatograph coupled to a Hewlett-Packard 5971A mass-selective detector, and product identities were confirmed by comparison with the NIST database.[31] The GC data were recorded on an Agilent 7890A gas chromatograph equipped with a HP-5 capillary column. Catalytic reactions and materials were performed and stored at room temperature (23 ± 2 °C).

Preparation of $Ru_2(esp)_2Cl$ (1a). $Ru_2(OAc)_4Cl$ (200 mg, 0.422 mmol) was added to a solution composed of 20 mL of H_2O and 30 mL of MeOH and stirred to dissolution at room temperature. H_2esp ligand (259 mg, 0.929 mmol, 2.2 equiv) was also dissolved in 10 mL of MeOH and added dropwise to the $Ru_2(OAc)_4Cl$ mixture. The reaction mixture was refluxed for 3 h before being cooled, and MeOH was removed under reduced pressure. The resulting precipitate was filtered, rinsed with water, and then redissolved in ethyl acetate. The ethyl acetate solution was washed three times with water and then once with brine. The organic phase was reduced in volume, placed on a short silica gel column, and eluted with EtOAc/hexanes (3:1). Collected product was dried over sodium sulfate, rotary-evaporated, and placed under a vacuum overnight to yield a golden burgundy solid (294 mg, 88.0% based on Ru). Product was recrystallized for elemental analysis in CH_2Cl_2 and dried under vacuum for 2 days. MS-FAB (m/e, based on ^{101}Ru) 756 [$M^+ - Cl$]. Anal. for $Ru_2(esp)_2Cl{\cdot}0.5CH_2Cl_2$, found (calcd): C 46.60 (46.65), H 5.37 (5.42). UV−vis−NIR, λ_{max} [nm, ε ($M^{-1}{\cdot}cm^{-1}$)] 467 (1030). μ_{eff} (295 K) = 3.84μ_B.

Preparation of $[Ru_2(esp)_2(H_2O)_2](BF_4)$ (1b). Compound **1b** was prepared by treating 302 mg of $Ru_2(esp)_2Cl$ in 25 mL of ethanol with 2 equiv of $AgBF_4$ (74 mg); formation of a white precipitate was observed upon addition of the silver salt. The reaction mixture was filtered to remove the silver chloride salt, and the filtrate was dried, redissolved in ethyl acetate, and washed with water. Upon slow evaporation of the organic phase in air, compound **1b** was obtained as an orange solid (187 mg, 62%). Product was recrystallized for elemental analysis in CH_2Cl_2 and dried under vacuum overnight. Anal. for $[Ru_2(esp)_2(H_2O)_2]BF_4$, found (calcd): C 44.22 (43.59), H 5.16 (5.49). UV−vis−NIR, λ_{max} [nm, ε ($M^{-1}{\cdot}cm^{-1}$)] 438 (937). μ_{eff} (295 K) = 3.60μ_B.

General Procedures for Catalytic Reactions. *In Solution.* Indicated amounts of catalyst and 1.25 mmol of the indicated sulfide were added to the indicated amount of solvent. TBHP was then added to the homogeneous solution to initiate the reaction. Aliquots (2−4 μL) of this solution were then diluted at the indicated time in 500 μL of , and 1 μL of this subsequent solution was injected immediately for GC/GC-MS analysis.

Solvent-Free Reactions. The indicated amount of catalyst (0.05 mol % with respect to the sulfide) was directly dissolved in 8 mmol of MPS and placed in an ice bath. Reactions were initiated by the addition of TBHP, and the solution was maintained in an ice bath for 15 min after its initiation before subsequent return to room temperature. Aliquots (5 μL) of this solution were then serially diluted at the indicated time in EtOAc and subsequent injected immediately for GC-MS analysis.

Variation of TBHP with Catalyst $Ru_2(esp)_2Cl$. Stock solutions of MPS (50 mM), TBHP (1000 mM), and $Ru_2(esp)_4Cl$ (0.60 mM) were made in CH_3CN. For each reaction, 400 μL of the MPS stock solution was added to a 10 mL volumetric flask with varied amounts of the TBHP solution. The solution was diluted to 10 mL with CH_3CN, and 3.0 mL was transferred to a cuvette. Reactions were initiated by the addition of 100 μL $Ru_2(esp)_2Cl$ solution, and the reactions were monitored at 290 nm for 35 min. All reactions were referenced to CH_3CN. Initiation times in the presence of $Ru_2(esp)_2Cl$ typically spanned 3−5 min; these lag periods were omitted from the data analysis.

Variation of TBHP with $Ru_2(OAc)_4Cl$ in CH_3CN/H_2O (1:1). Stock solutions of 50 mM MPS, 1000 mM TBHP, and 0.60 mM $Ru_2(OAc)_4Cl$ were prepared in CH_3CN/H_2O (1:1). To make the appropriate mixture for each reaction, 400 μL of MPS stock solution was added to a 10 mL volumetric flask with varied amounts of TBHP and diluted with CH_3CN/H_2O (1:1). Of this mixture, 3.0 mL was added to a cuvette and the reactions were initiated by addition of 100 μL of 0.60 mM $Ru_2(OAc)_4Cl$ stock solution. Reactions were monitored for 30 min at 290 nm and were referenced to CH_3CN/H_2O (1:1).

Variation of $Ru_2(esp)_2Cl$ in CH_3CN. An aliquot (3.0 mL) of stock solution that was 2 mM in MPS and 200 mM in TBHP in CH_3CN was added to a cuvette. Aliquots of 0.60 mM stock solution of $Ru_2(esp)_2Cl$ in CH_3CN were then added to the cuvette, mixed thoroughly for less

dx.doi.org/10.1021/ic401588j | Inorg. Chem. 2013, 52, 12545−12552

than 5 s, and immediately monitored at 290 nm for 35 min. Each reaction was referenced to CH_3CN.

Variation of $Ru_2(OAc)_4Cl$ in CH_3CN/H_2O (1:1). An aliquot (3.0 mL) of stock solution that was 2 mM in MPS and 200 mM in TBHP in CH_3CN/H_2O (1:1) was added to a cuvette. An aliquot (33.3, 66.7, 100, 133.3, 167.7, 200, 233.3, 267.7, or 300 μL) of a 0.6 mM stock solution of $Ru_2(OAc)_4Cl$ in CH_3CN/H_2O (1:1) was added to the cuvette for each reaction, respectively, mixed thoroughly for less than 5 s, and immediately monitored at 290 nm for 30 min. Resulting plots of $\ln(Abs_{290})$ were linear for the spectra obtained. Each reaction was referenced to a solution containing 200 mM TBHP in CH_3CN/H_2O (1:1).

Hammett Plots with $Ru_2(OAc)_4Cl$ and $Ru_2(esp)_2Cl$. Stock solutions of 4 mM sulfides [thioanisole (MPS), methyl *p*-tolyl sulfide, 1-methoxy-4-(methylthio)benzene, 4-bromophenyl methyl sulfide, 4-chlorophenyl methyl sulfide, and 4-(methylthio)benzonitrile] were made in CH_3CN. A stock solution of TBHP (400 mM) was dissolved in CH_3CN. Catalyst stock solutions were made for $Ru_2(OAc)_4Cl$ (1.8 mM) in CH_3CN/H_2O (1:1) and $Ru_2(esp)_2Cl$ (1.8 mM) in CH_3CN, respectively. In each reaction, 0.75 mL of the indicated sulfide stock solution was added to 2.25 mL of the TBHP stock solution in a cuvette. Catalyst stock solution was then added to initiate the reaction, which was monitored at 290 nm until a baseline was obtained. All reactions were referenced to CH_3CN. Resulting plots of ln(Abs290) were linear for at least the first half of the reaction. Equation 1 was again applied to yield the values for k_{obs} for each run, correcting for the differences in absorbance for different substrates. After elimination of the first 5 min of data analysis, the $\ln(Abs_{290,corr})$ plot was linear for the first half of the decay curve.

Computational Details. Theoretical calculations were performed on the hypothetical compound **2′**·TBHP with Gaussian 03.[32] Geometry optimizations were performed with the generalized gradient approximation, with Becke's nonlocal correction to exchange and Perdew's nonlocal correction to correlation (BP86).[33] The basis set used was the LanL2DZ effective core potential[34] for the metal centers and 6-31G (d,p)[35] for the ligand atoms. No negative frequency was observed in the vibrational frequency analysis.

X-ray Crystallography. Single crystals of $[Ru_2(esp)_2(H_2O)_2]BF_4$ (**1b**) were grown via slow diffusion of hexanes into a $EtOAc/CH_2Cl_2$ solution of **1b**. A dark red crystal of **1b** of dimensions 0.31 × 0.29 × 0.12 mm^3 was mounted in a quartz capillary with the mother liquor. X-ray intensity data was measured on a Bruker SMART1000 CCD-based X-ray diffractometer system by use of Mo Kα (λ = 0.710 73 Å) at 300 K. Bruker SHELXTL (version 5.1) software package was utilized to solve the crystal structure.[36] The direct method was used to determine the positions of all non-hydrogen atoms. In addition to **1b**, the asymmetric unit also contains one ethyl acetate solvent molecule. The structure was refined to convergence by least-squares method on F^2, SHELXL-93, incorporated in SHELXTL.PC V 5.03. Crystal data for $[Ru_2(esp)_2(H_2O)_2]BF_4$·EtOAc: $C_{36}H_{52}BF_4O_{12}Ru_2$, FW = 965.73, monoclinic, $P2_1/n$, a = 9.7724(4), b = 24.1791(9), c = 18.0905(7) Å, β = 96.535(1)°; V = 4246.8(3) $Å^3$, Z = 2, D_{calcd} = 1.510 g·cm^{-3}. Of 22 310 reflections measured, 7479 were unique (R_{int} = 0.025). Least-squares refinement based on 7479 reflections with $I \geq 2\sigma(I)$ and 509 parameters led to convergence with final $R1$ = 0.037 and $wR2$ = 0.098.

■ ASSOCIATED CONTENT

Supporting Information

X-ray crystallographic details of **1b** (CIF); additional text, four figures, and three tables with optimized model structures, solvent-free reaction results and linear dependence of initial rate on concentration of **1b** and **2**, and additional DFT optimization for $S = {}^1/_2$ ground state (PDF). This material is available free of charge via the Internet at http://pubs.acs.org.

■ AUTHOR INFORMATION

Corresponding Author

*E-mail: tren@purdue.edu.

Notes

The authors declare no competing financial interest.

■ ACKNOWLEDGMENTS

We gratefully acknowledge financial support from the Army Research Office (Grants DAAD 190110708 and W911NF-06-1-0305). T.R. acknowledges IR/D support from the National Science Foundation during the preparation of this Article, and L.V. was supported in part by an AGEP supplement from the National Science Foundation (CHE 1057621).

■ REFERENCES

(1) (a) Carreno, M. C. *Chem. Rev.* **1995**, *95*, 1717−1760. (b) Carreño, M. C.; Hernández-Torres, G.; Ribagorda, M.; Urbano, A. *Chem. Commun.* **2009**, 6129−6144.
(2) Babich, I. V.; Moulijn, J. A. *Fuel* **2003**, *82*, 607−631.
(3) (a) Wagner, G. W.; Yang, Y. C. *Ind. Eng. Chem. Res.* **2002**, *41*, 1925−1928. (b) Smith, B. M. *Chem. Soc. Rev.* **2008**, *37*, 470−478. (c) Kim, K.; Tsay, O. G.; Atwood, D. A.; Churchill, D. G. *Chem. Rev.* **2011**, *111*, 5345−5403.
(4) Barker, J. E.; Ren, T. *Tetrahedron Lett.* **2004**, *45*, 4681−4683.
(5) Phan, T. D.; Kinch, M. A.; Barker, J. E.; Ren, T. *Tetrahedron Lett.* **2005**, *46*, 397−400.
(6) Barker, J. E.; Ren, T. *Tetrahedron Lett.* **2005**, *46*, 6805−6808.
(7) Villalobos, L.; Cao, Z.; Fanwick, P. E.; Ren, T. *Dalton Trans.* **2012**, *41*, 644−650.
(8) Lee, H. B.; Ren, T. *Inorg. Chim. Acta* **2009**, *362*, 1467−1470.
(9) Oae, S.; Doi, J. T. *Organic Sulfur Chemistry: Structure and Mechanism*; CRC Press: Boca Raton, FL, 1991.
(10) Kuhnen, L. *Angew. Chem., Int. Ed. Engl.* **1966**, *5*, 893.
(11) Wang, Y.; Lente, G.; Espenson, J. H. *Inorg. Chem.* **2002**, *41*, 1272−1280.
(12) (a) Ratnikov, M. O.; Doyle, M. P. *J. Am. Chem. Soc.* **2013**, *135*, 1549−1557. (b) Ratnikov, M. O.; Farkas, L. E.; McLaughlin, E. C.; Chiou, G.; Choi, H.; El-Khalafy, S. H.; Doyle, M. P. *J. Org. Chem.* **2011**, *76*, 2585−2593. (c) Catino, A. J.; Forslund, R. E.; Doyle, M. P. *J. Am. Chem. Soc.* **2004**, *126*, 13622−13623. (d) Catino, A. J.; Nichols, J. M.; Choi, H.; Gottipamula, S.; Doyle, M. P. *Org. Lett.* **2005**, *7*, 5167−5170. (e) Choi, H.; Doyle, M. P. *Org. Lett.* **2007**, *9*, 5349−5352. (f) McLaughlin, E. C.; Choi, H.; Wang, K.; Chiou, G.; Doyle, M. P. *J. Org. Chem.* **2009**, *74*, 730−738.
(13) Barker, J. E.; Ren, T. *Inorg. Chem.* **2008**, *47*, 2264−2266.
(14) Stephenson, T. A.; Wilkinson, G. *J. Inorg. Nucl. Chem.* **1966**, *28*, 2285−2291.
(15) Espino, C. G.; Fiori, K. W.; Kim, M.; Du Bois, J. *J. Am. Chem. Soc.* **2004**, *126*, 15378−15379.
(16) Aquino, M. A. S. *Coord. Chem. Rev.* **1998**, *170*, 141−202.
(17) Miskowski, V. M.; Gray, H. B. *Inorg. Chem.* **1988**, *27*, 2501−2506.
(18) Dequeant, M. Q.; Fanwick, P. E.; Ren, T. *Inorg. Chim. Acta* **2006**, *359*, 4191−4196.
(19) Drysdale, K. D.; Beck, E. J.; Cameron, T. S.; Robertson, K. N.; Aquino, M. A. S. *Inorg. Chim. Acta* **1997**, *256*, 243−252.
(20) Vassell, K. A.; Espenson, J. H. *Inorg. Chem.* **1994**, *33*, 5491−5498.
(21) Pilling, M. J.; Seakins, P. W. *Reaction Kinetics*, 3rd ed.; Oxford University Press.: New York, 2002.
(22) (a) Duboc-Toia, C.; Ménage, S.; Ho, R. Y. N.; Que, L.; Lambeaux, C.; Fontecave, M. *Inorg. Chem.* **1999**, *38*, 1261−1268. (b) Mekmouche, Y.; Hummel, H.; Ho, R. Y. N.; Que, J., L.; Schünemann, V.; Thomas, F.; Trautwein, A. X.; Lebrun, C.; Gorgy, K.; Leprêtre, J.-C.; Collomb, M. N.; Deronzier, A.; Fontecave, M.; Ménage, S. *Chem.—Eur. J.* **2002**, *8*, 1196−1204.
(23) (a) Bateman, L.; Hargrave, K. R. *Proc. R. Soc. London, A* **1954**, *224*, 399−411. (b) Bateman, L.; Hargrave, K. R. *Proc. R. Soc. London, A* **1954**, *224*, 389−398.
(24) Hansch, C.; Leo, A.; Taft, R. W. *Chem. Rev.* **1991**, *91*, 165.

(25) Acquaye, J. H.; Muller, J. G.; Takeuchi, K. J. *Inorg. Chem.* **1993**, *32*, 160−165.
(26) Angaridis, P. Ruthenium Compounds. In *Multiple Bonds between Metal Atoms*, 3rd ed.; Cotton, F. A., Murillo, C. A., Walton, R. A., Eds.; Springer Science and Business Media: New York, 2005.
(27) Kosnikov, A. Y.; Antonovskii, V. L.; Lindeman, S. V.; Antipin, M. Y.; Struchkov, Y. T.; Turovskii, N. A.; Zyat'kov, I. P. *Theor. Exp. Chem.* **1989**, *25*, 73−77.
(28) Ren, T. *Organometallics* **2005**, *24*, 4854−4870.
(29) Long, A. K. M.; Timmer, G. H.; Pap, J. S.; Snyder, J. L.; Yu, R. P.; Berry, J. F. *J. Am. Chem. Soc.* **2012**, *133*, 13138−13150.
(30) Armarego, W. L. F.; Perrin, D. D. In *Purification of Laboratory Chemicals*, 4th ed.; Butterworth−Heinemann: Oxford, U.K., 1996.
(31) NIST98 and Search Program v 1.7, C. S. Inc. 1999.
(32) Frisch, M. J.; Trucks, G. W.; Schlegel, H. B.; Scuseria, G. E.; Robb, M. A.; Cheeseman, J. R.; Montgomery, J. A., Jr.; Vreven, T.; Kudin, K. N.; Burant, J. C.; Millam, J. M.; Iyengar, S. S.; Tomasi, J.; Barone, V.; Mennucci, B.; Cossi, M.; Scalmani, G.; Rega, N.; Petersson, G. A.; Nakatsuji, H.; Hada, M.; Ehara, M.; Toyota, K.; Fukuda, R.; Hasegawa, J.; Ishida, M.; Nakajima, T.; Honda, Y.; Kitao, O.; Nakai, H.; Klene, M.; Li, X.; Knox, J. E.; Hratchian, H. P.; Cross, J. B.; Bakken, V.; Adamo, C.; Jaramillo, J.; Gomperts, R.; Stratmann, R. E.; Yazyev, O.; Austin, A. J.; Cammi, R.; Pomelli, C.; Ochterski, J. W.; Ayala, P. Y.; Morokuma, K.; Voth, G. A.; Salvador, P.; Dannenberg, J. J.; Zakrzewski, V. G.; Dapprich, S.; Daniels, A. D.; Strain, M. C.; Farkas, O.; Malick, D. K.; Rabuck, A. D.; Raghavachari, K.; Foresman, J. B.; Ortiz, J. V.; Cui, Q.; Baboul, A. G.; Clifford, S.; Cioslowski, J.; Stefanov, B. B.; Liu, G.; Liashenko, A.; Piskorz, P.; Komaromi, I.; Martin, R. L.; Fox, D. J.; Keith, T.; Al-Laham, M. A.; Peng, C. Y.; Nanayakkara, A.; Challacombe, M.; Gill, P. M. W.; Johnson, B.; Chen, W.; Wong, M. W.; Gonzalez, C.; Pople, J. A. *Gaussian 03, Revision D.02*; Gaussian, Inc.: Wallingford, CT, 2003.
(33) (a) Becke, A. D. *Phys. Rev. A* **1988**, *38*, 3098−3100. (b) Perdew, J. P. *Phys. Rev. B* **1986**, *33*, 8822−8824.
(34) Wadt, W. R.; Hay, P. J. *J. Chem. Phys.* **1985**, *82*, 284−298.
(35) (a) Ditchfie, R.; Hehre, W. J.; Pople, J. A. *J. Chem. Phys.* **1971**, *54*, 724. (b) Hehre, W. J.; Ditchfie, R.; Pople, J. A. *J. Chem. Phys.* **1972**, *56*, 2257.
(36) Sheldrick, G. M. *Acta Crystallogr. A* **2008**, *64*, 112−122.